Nix, A. R., & Athanasiadou, G. E. (2000). Investigation into the sensitivity of the power predictions of a microcellular ray tracing propagation model. IEEE Transactions on Vehicular Technology, 49(4), 1140 - 1151. [4]. 10.1109/25.875221

Investigation into the Sensitivity of the Power Predictions of a Microcellular Ray Tracing Propagation Model

Georgia E. Athanasiadou, *Member, IEEE,* and Andrew R. Nix, *Associate Member, IEEE*

***Abstract*—This paper investigates the sensitivity of the three-dimensional (3-D) ray tracing microcellular model presented in [1], [2]. The variation of the received power is examined for different ray permutations, wall characteristics, antenna position offsets and database inaccuracies. Predictions of the different configurations in line-of-sight (LOS), non-LOS (NLOS), and deep shadow areas are compared with each other and also with narrowband measurements. The analysis illustrates that although the model produces reliable results with five orders of reflection and one order of diffraction, higher orders of reflection and double diffracted rays enhance the model's performance in deep shadow areas. It is also shown that good agreement with measured results can be obtained for wall conductivity in the order of 10^{-3} S/m and values of relative permitivity around five. The sensitivity analysis to the antenna positioning and database inaccuracies indicates that the receiver positions which suffer the highest power deviations are those at the boundaries of the LOS areas, as well as the positions in the deep shadow regions. In general, for antenna offsets up to 1 m, the predictions of the model are not significantly affected. Finally, the building databases with 1m maximum displacement do not have severe effects on the predictions, but databases with less accuracy can seriously degrade the performance of the model.**

***Index Terms*—Building databases, material characteristics, propagation modelling, radio channel predictions, ray tracing, sensitivity analysis.**

I. Introduction

DURING the last decade, ray tracing has emerged as the dominant technique for small cell propagation modeling. Naturally, two of the most critical issues related to all propagation models are accuracy and sensitivity of their predictions. Building upon work previously presented in [1]–[3] about the ray tracing algorithm and its accuracy, this paper investigates the sensitivity of the narrowband predictions to various input parameters. The sensitivity analysis enables the user to configure the propagation model correctly, and hence, obtain accurate results. It provides valuable information about the impact of each of the simulation parameters and the obtainable prediction accuracy, given the margins of the input parameters. Despite the growing interest on ray based algorithms, the published work on the sensitivity of the predictions of these models is limited [4]–[7].

The ray tracing algorithm employed in this paper is based on the theory of images. The model allows the rapid generation of complex channel impulse response characteristics, and can evaluate scenarios incorporating many thousands of objects by utilizing the concept of "illumination zones." In the model the object database is held in two dimensions but the ray-tracing engine operates in three dimensions. The base station and the mobiles are assumed to remain below roof top height and based on this assumption, the buildings are modeled as infinitely tall. However, the antenna heights are specified and the ground is also considered. The rays are traced in three-dimensional (3-D) space and all reflections, transmissions and diffractions are computed using 3-D vector mathematics. This hybrid analysis allows factors such as polarization and 3-D antenna patterns to be fully considered. (For a more detailed description of the model, see [1] and [2]. For more references on ray tracing models, see the works cited in [1]–[7], [9], and [11].)

In Section II, the measurements used for the sensitivity analyses are presented. The variation of the received power is examined for different orders of reflection and diffraction in Section III, and for various wall characteristics in Section IV. Section V examines the predictions for 23 transmitter positions around the original antenna location. Finally, Section VI investigates the effects that the database inaccuracies have on the power results by studying 40 different scenarios. The analyses are performed for LOS, NLOS, and also deep shadow areas where energy can only reach through multiple reflected and diffracted rays.

II. Measurements and Model Set-Up

The narrowband measurements used in this paper were performed in central Bristol, U.K. [8]. The measurement site, the examined transmitter position and the test route are depicted in Fig. 1. The transmitted power was 30 dBm (including the cable and antenna losses) at 1.823 GHz. Typical half wavelength vertically polarized dipoles, mounted below the roof height of adjacent buildings were used at both ends of the radio link. The transmitting antenna was on a mast at a height of 5 m above the ground level. The receiver was at a height of 1.57 m, mounted on a trolley which was slowly and carefully moved along the predefined route. The narrowband receiver recorded field strength against distance from the starting point, with a spatial sampling

Manuscript received December 3, 1998; revised June 11, 1999. The measurements and the sensitivity analysis shown in this paper were supported in part by British Telecom as part of the Virtual University Research Initiative (VURI) project. This work was performed while G. E. Athanasiadou was with the Centre for Communications Research, University of Bristol, U.K.

G. E. Athanasiadou is with Adaptive Broadband Ltd., The Westbrook Centre, Cambridge CB4 1YG, U.K. (e-mail: gathanasiadou@hotmail.com).

A. R. Nix is with the Centre for Communications Research at the University of Bristol, U.K. (e-mail: andy.nix@bristol.ar.uk).

Publisher Item Identifier S 0018-9545(00)04822-2.

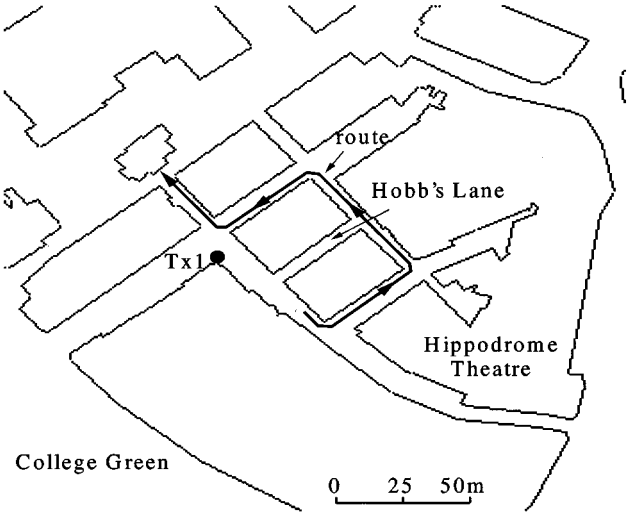

Fig. 1. Microcellular map of the measurement area.

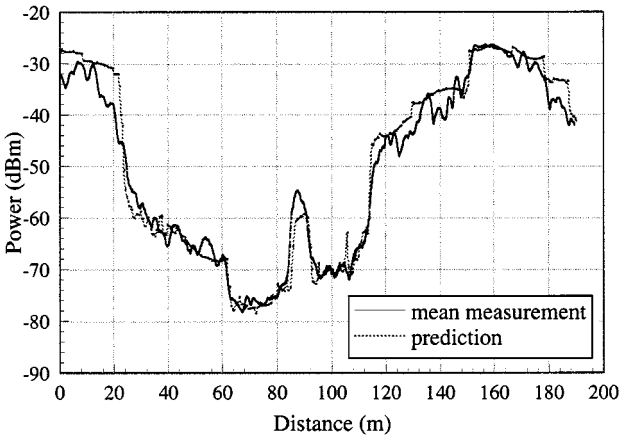

Fig. 2. Model's prediction against mean measurement for transmitter position $T \times 1$.

rate of 4 cm. The fast fading was extracted from the measured results with a sliding rectangular window averaging process. A 10 wavelength window (equivalent to 1.67 m) was chosen, so that the results maintain their site specific information as much as possible. Three measurement runs were performed along the same route and with the same configuration. For more representative results and in order to remove localized temporal effects, the slow fading envelopes were averaged to produce a mean envelope. It was noticed that there was a high degree of correlation between the various runs, although some of them were taken on different days [8]. The RMS error of each of the measured envelopes with respect to the mean envelope was as high as 3.45 dB and the total RMS error was 2.69 dB. These numbers illustrate how repeatable and representative the measurements are for the route under study. Since it is not reasonable to expect the prediction tools to reproduce the measurements with more accuracy than their own repeatability, these values set the upper limit of attainable accuracy of a propagation model in that environment.

The building database of the measurement site (part of which is shown in Fig. 1) was extracted from the U.K. Ordinance Survey "Landline" database. The digital map was then pre-processed to remove any redundant information (e.g., internal walls), and diffraction corners were automatically added. The simulated area is approximately 500×500 m^2 and contains 438 external walls. The walls and the ground are modeled as smooth, and with the same electrical properties ($\varepsilon_r = 5, \sigma = 0.005$ S/m). The wall thickness is 0.6 m. Unlike the field trials, the spatial resolution between the prediction points is 0.5 m. This is because the predicted received power, which is produced from the summation of the power of the rays reaching the receiver, is inherently time averaged and no further action is needed in order to remove the fast fading. Unless otherwise stated, for the results presented in this paper all rays with up to seven orders of reflection and one order of diffraction are traced, and the model's parameters are as described in this paragraph.

Fig. 2 depicts the mean measurement and the prediction along the predefined route. The starting point of the route is at a LOS position about 50 m away from the transmitting antenna. When the receiver turns left and moves into NLOS positions, the mean signal level decreases significantly (more than 20 dB, at $\sim$20 m). As it turns into the second corner and enters a deep shadow region, a further drop (less than 10 dB, at $\sim$60 m) is evident. An increase in power of at least 18 dB ($\sim$86 m) happens across the end of Hobb's Lane (see Fig. 1), which acts as a street canyon for the transmitted electromagnetic waves. As the mobile re-enters the deep shadow area, the power falls again, however higher signal levels are measured since the distance between the two antennas has been reduced. When the receiver turns left and enters less shadowed areas ($\sim$118 m), the signal increases by about 15 dB and keeps increasing as the trolley approaches the second LOS section of the route. The transition from NLOS to LOS ($\sim$157 m) is not as dramatic (approximately 10 dB increase) because the two antennas are already very close and strong reflections have already raised the mean signal strength. The measured power falls slowly as the receiver moves away from the transmitter and finally re-enters a NLOS area near the end of the route. Obviously, because the power changes are site dependent, there is no simple rule for the degree of variation of the signal level as the receiver moves into or out of LOS, NLOS, or deep shadow areas. The simulation results shown in Fig. 2 are for nine reflections and two diffractions and agree very well with the measurement trend, remaining very close to the measured values for the majority of the route positions. Their mean and RMS difference are 1.07 dB and 3.37 dB, respectively. (Note that the errors in this paper are calculated with all values in the logarithmic scale.)

III. Sensitivity of the Power Predictions to the Maximum Permitted Ray Interactions with the Envitonment

As described in [1] and [2], the basic propagation mechanisms used by the model are specular reflection, corner diffraction and wall transmission. This section investigates the sensitivity of the microcellular propagation model to the maximum permitted orders of reflection and diffraction. Although wall transmitted rays are also supported, this propagation mechanism is generally ignored for outdoor microcellular studies and only

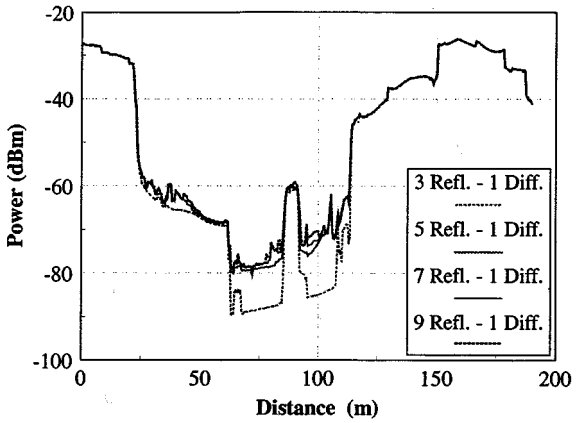

Fig. 3. Power predictions considering different number of maximum allowed reflections.

TABLE I
ERRORS OF THE POWER RESULTS CONSIDERING VARIOUS ORDERS OF REFLECTION AND 1 ORDER OF DIFFRACTION WITH RESPECT TO THE PREDICTIONS FOR NINE REFLECTIONS AND ONE DIFFRACTION

	Mean error (dB)	RMS error (dB)
3 refl. - 1 diff.	-3.09	5.71
5 refl. - 1 diff.	-0.53	1.18
7 refl. - 1 diff.	-0.14	0.43

TABLE II
ERROR STATISTICS OF THE PREDICTIONS COSIDERING VARIOUS ORDERS OF REFLECTION AND 1 ORDER OF DIFFRACTION WITH RESPECT TO THE MEASURED RESULTS

	Mean error (dB)	RMS error (dB)
3 refl. - 1 diff.	-2.25	7.17
5 refl. - 1 diff.	0.32	3.84
7 refl. - 1 diff.	0.71	3.53
9 refl. - 1 diff.	0.85	3.48

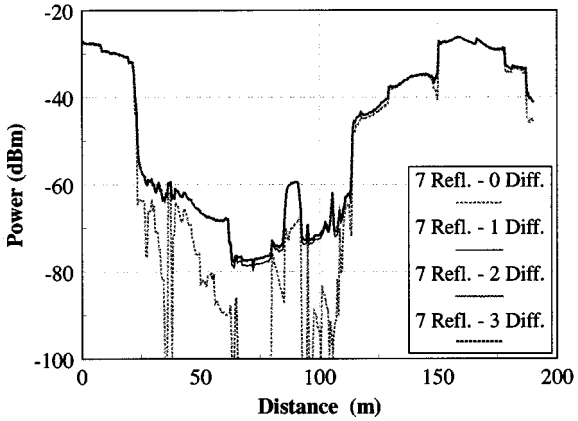

Fig. 4. Power predictions for different orders of corner diffraction.

used in order to predict outdoor-to-indoor and indoor-to-outdoor coverage.

A. Sensitivity to the Maximum Permitted Order of Reflection

In this section, simulation results are compared for three, five, seven, and nine orders of reflection, together with one order of diffraction. It has to be mentioned that these are wall reflections, i.e., the ground reflection is not considered here as an extra order of reflection [1]. As depicted in Fig. 3, in LOS regions the signal level is the same for all the above ray permutations. In these areas the received power is determined by a few rays; the direct together with some strong rays with only one or two orders of reflection. Compared with these dominant rays, the contributions from the rays with higher orders of reflection are not significant enough to change the total power under LOS conditions. As the mobile enters NLOS areas where the previously dominant rays cannot reach, higher orders of reflections are needed in order to obtain accurate power predictions. The more shadowed the NLOS area, the more reflections are required for the power results to converge to their final values. In the deep shadow areas between the second and third corner of the route (between $\sim$62 and 115 m in Fig. 3), as the number of reflections increases from 3 to 5, the predictions improve dramatically. In this region, the difference between the power values for the highest (9) and the lowest (3) permitted orders of reflection is 9.6 dB on average, while at some points, it is as high as 21.5 dB.

Table I provides the error statistics of the above predictions with respect to the received power with the maximum studied order of reflection (9). It can be seen that the error decreases with the increase of the number of reflections, since the simulation results for each position tend to converge to a value after a certain order of reflection. The RMS difference between the simulation results obtained for nine and five orders of reflection is 1.18 dB. However, these predictions deviate as much as 8.2 dB at certain NLOS points (between $\sim$80 and 100 m in Fig. 3). Although with seven reflections the predictions have not quite reached their converged value at several mobile positions in the deep shadow area, the RMS difference between the simulation results for seven and nine reflections is only 0.43 dB. In Table II are shown the error statistics of the results with the above model configurations in comparison with the mean measurement along the same route. With five or more reflections, the RMS error is below 4 dB and decreases with the increasing number of reflections, while the mean error is less than 1 dB.

B. Sensitivity to the Maximum Permitted Order of Diffraction

The importance of the corner diffraction in the modeling of outdoor scenarios is demonstrated in this section. Simulation results with 0, 1, 2, and 3 maximum orders of diffraction, together with seven orders of reflection are compared with each other and with the narrowband measurements. Generally, diffraction attenuates the power of a ray much more than a reflection, and at the same time increases the complexity of the model enormously. However, as illustrated in Fig. 4, it is a very significant propagation mechanism for the study of outdoor scenarios (see [4], too). When no diffractions are allowed, only the power of the LOS areas can be predicted, while for long sections of the route, no rays reach the mobile, even after seven orders of

TABLE III
ERRORS OF THE POWER RESULTS CONSIDERING VARIOUS ORDERS OF DIFFRACTION AND 7 ORDERS OF REFLECTION WITH RESPECT TO THE PREDICTIONS FOR SEVEN REFLECTIONS AND THREE DIFFRACTIONS

	Mean error (dB)	RMS error (dB)
7 refl. - 0 diff.	-13.47	27.20
7 refl. - 1 diff.	-0.28	0.50
7 refl. - 2 diff.	-0.02	0.08

TABLE IV
ERROR STATISTICS OF THE PREDICTIONS CONSIDERING VARIOUS ORDERS OF DIFFRACTION AND 7 ORDERS OF REFLECTION WITH RESPECT TO THE MEASURED RESULTS

	Mean error (dB)	RMS error (dB)
7 refl. - 0 diff.	-12.52	27.98
7 refl. - 1 diff.	0.71	3.53
7 refl. - 2 diff.	0.97	3.40
7 refl. - 3 diff.	0.99	3.40

reflection (e.g., between 65.5 and 79.5 m). Moreover in areas where strong reflections exist, diffraction affects the predictions by making the transition smoother from LOS to NLOS areas and in and out of the illuminated areas of strong reflections (between ~115 and 150 m and also from ~179 m and onwards).

As it can be seen in Fig. 4, the simulation results reach their converged values at all positions, with two orders of diffraction. The maximum difference between the power predictions with one and three orders of diffraction is 1.55 dB. The RMS difference between the results with three orders and those with 1 and 2 is less than 0.6 dB (Table III). As shown in Table IV, the errors of the predictions for one to three orders of diffraction compared with the measurements, are almost the same (in all three cases the RMS errors are ~3.5 dB). Although triple diffracted rays could reach deep shadow areas far away from the transmitter, they would be very weak to be considered. At the positions where only rays with three orders of diffraction could reach, roof top diffracted rays should dominate since they would reach most positions with up to two diffractions and multiple reflections. Nevertheless, these areas are most likely to be outside the coverage limits of a microcell. Hence, three orders of corner diffraction are too many for a typical coverage study, while with two orders of diffraction the model produces reliable predictions even in the deep shadow areas of the microcell.

C. Number of Traced Rays

In order to ideally model an outdoor environment, a very large number of ray interactions with the environment should be considered. This would increase the complexity and the running time enormously. However, what is most encouraging is that after a certain number of reflections and diffractions, the model's predictions at each point converge to a value, and the addition of extra orders does not affect the results. Hence, the radio channel can be modeled if sufficient number of ray interactions with the environment are considered.

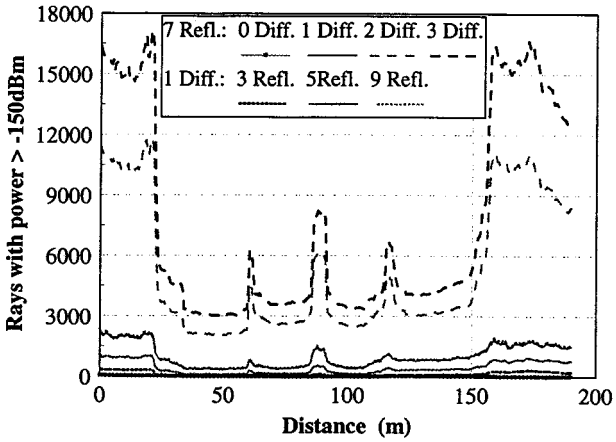

Fig. 5. The number of traced rays (with power >-150 dBm) for different ray permutations.

Fig. 5 shows the number of rays detected by the model for different ray permutations and with power greater than -150 dBm. This is only a subtotal of the actual number of the traced rays at each position, since valid rays with power less than the predefined power threshold are not considered. As expected, more rays are traced by the model as the maximum permitted interactions with the environment rises. The mean number of rays increases from 122 to 1037 as the reflections rise from three to nine, with one order of diffraction. When three, five, and seven orders of reflection and 1 diffraction are considered in the study, the rays found are 9.32, 37.89, and 94.15%, respectively, of those traced when up to nine reflections and one diffraction are permitted in the model.

However, what is really striking is the complexity that each extra order of diffraction adds to the model. Unlike reflections which only have a limited illumination zone (most of the time much smaller than their 180° maximum angular width), each illuminated diffraction corner acts as a secondary source which launches rays in almost all directions [1]. Each additional order of diffraction increases the flexibility of the rays and as a result, raises dramatically the total number of generated images seven reflections and zero, one, two, and three orders of diffraction, the mean number of rays along the route is 15, 984, 5234, and 7534, respectively, while for the same interactions, the maximum number of rays is 52, 2302, 11 756, and 17 135, respectively. Most of these rays are very weak and do not contribute to the channel characterization, while the strong and most significant ones are only a small portion of the traced rays. Permitting up to seven orders of reflections and two diffractions, the number of rays found with power greater than -150 dBm are depicted in Fig. 6, together with the number of rays with power inside a 30 dB window from the strongest ray at each point. There is obviously a disproportional relation between these two numbers. In LOS areas where the model can trace many thousands of rays, only a few of them (less than 0.5%) are really important. As the mobile enters into NLOS areas where less powerful rays exist, the power levels fall and more rays are included

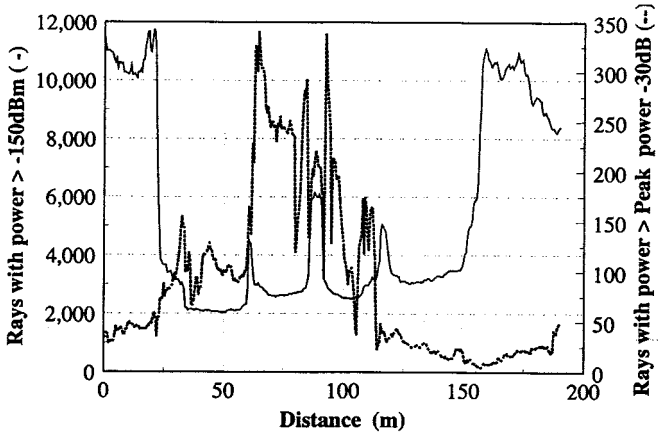

Fig. 6. Total number of rays (considering seven reflections and two diffractions) together with the number of rays inside a 30 dB window from the strongest ray.

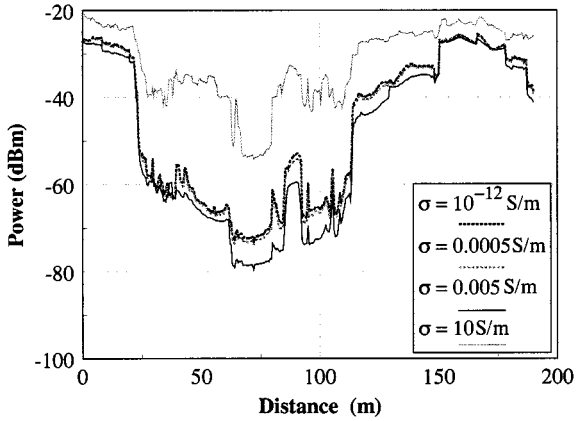

Fig. 7. Power predictions for various values of wall conductivity.

in the 30 dB power window. In the best case, just 11.1% (340 rays) of the traced rays have power inside the 30 dB window from the strongest ray.

Although at each point only a few of the traced rays contribute to the channel characterization, it is important that the model can handle a very large number of rays, in order to produce reliable results for complex environments, even in deep shadow areas away from the transmitter. Criteria based on power can limit the total number of rays considered at a certain point (and hence significantly speed up the model), but not the total number of the generated images. This is because a ray that is insignificant compared to the other beams illuminating the same region, can be very important for another area where powerful rays cannot reach. This ray can also be reflected or diffracted and produce vital rays for the channel characterization at other receiver locations or even the same position, if the antenna radiation patterns are not omnidirectional. Moreover, an image that generates a relatively weak ray at a certain position, can produce a very strong path a few meters away, since the incident angles can change and hence, the corresponding reflection and diffraction coefficients also change. For the wideband characterization of the channel, even more rays must be taken into account. In that case, a ray can only be ignored if it is very small in comparison with the other rays in the same time bin, and if, together with the other rays with similar delays, cannot reach the power threshold of the analysis.

For all these reasons, it is difficult to simplify the image tree based on power criteria, without compromising the accuracy. Many potential rays (i.e., images) are needed in order to obtain accurate results, even in deep shadow areas away from the transmitter. The outdoor model investigated here, is capable of handling a large number of rays and supports the wideband, as well as the narrowband, characterization of complex microcellular environments [1].

IV. Sensitivity of the Power Predictions to the Wall Characteristics

Apart from its position, each wall in the building database is also characterized by its conductivity (σ), permitivity (ε_r) and thickness. These parameters directly affect the total reflection coefficient of the walls (see [9]), while the diffraction coefficients are indirectly affected through the reflection coefficients of the walls of the corners [10]. Wall thickness mainly influences the transmission coefficients and it is not examined in this paper. In the case of buildings with thick external walls, the reflection coefficients are predominantly determined by the ray which reflects off the exterior surface of the wall.

Individual building material data is not currently provided with the databases, since they are normally generated from aerial photography. General information about the building type (modern, Victorian, etc.) is the best that can be hoped for, without a site survey. All walls in the ray tracing models are usually represented by a single bulk set of parameters. Because of the variety of materials that exist in an area, the input parameters for the wall characteristics should not be those of one specific material, but the characteristics which can represent the whole environment [11]. Field trials at the examined area, or similar regions, are useful in order to calibrate the model to a specific type of environment. However, although the single bulk set of parameters is very convenient, a more selective characterization (e.g., for large metallic surfaces) is also possible in the employed model and would increase its accuracy. In order to analyze how the predictions are affected by the simulated wall characteristics, all the simulated objects are characterized by the same set of values ($\varepsilon_r = 5, \sigma = 0.005$ S/m) and by changing one of these values at a time, the model's sensitivity to that parameter is evaluated.

A. Sensitivity to the Conductivity of the Walls

First, the behavior of the model is examined as the values of conductivity range from 10^{-12} S/m to 10 S/m (Fig. 7). Although the conductivity of most building materials is in the order of 10^{-4} to 10^{-3} S/m (e.g., stone and brick), the conductivities of materials like glass and metal, which are also frequently encountered in the outdoor environments, significantly deviate from these values [12], [13]. As depicted in Fig. 7, while the conductivity remains relatively low (10^{-12}–0.0005 S/m), the power predictions do not change considerably. The RMS difference between the results with very low conductivity ($\sigma = 10^{-12}$ S/m) and those with $\sigma = 0.0005$ S/m is just 0.71 dB, while their maximum difference along the route is 2.13 dB. By further increasing the conductivity by one order of magnitude

TABLE V
ERROR STATISTICS OF THE POWER RESULTS CONSIDERING VARIOUS WALL CONDUCTIVITIES WITH RESPECT TO THE PREDICTIONS FOR $\sigma = 5 * 10^{-3}$ S/m

	Mean error (dB)	RMS error (dB)
$\sigma = 10^{-12}$ S/m	3.26	4.13
$\sigma = 5*10^{-4}$ S/m	2.66	3.44
$\sigma = 10$ S/m	17.80	20.75

TABLE VI
ERROR STATISTICS OF THE PREDICTIONS CONSIDERING VARIOUS WALL CONDUCTIVITIES WITH RESPECT TO THE MEASURED RESULTS

	Mean error (dB)	RMS error (dB)
$\sigma = 10^{-12}$ S/m	3.97	5.25
$\sigma = 5*10^{-4}$ S/m	3.37	4.76
$\sigma = 5*10^{-3}$ S/m	0.71	3.53
$\sigma = 10$ S/m	18.52	20.64

($\sigma = 0.005$ S/m), a considerable drop in the received signal levels appears in the results. The power decrease is 2.66 dB on average, but at certain mobile positions it is as high as 10.56 dB. The power differences are more obvious in the deep shadow areas where only multi-reflected rays exist. Each time a ray reflects off a wall, the power deviation due to the various reflection coefficients, increases. As a result, in the case of multi-reflected rays the difference accumulates and becomes noticeable. As the walls become more conductive ($\sigma = 10$ S/m), the channel characteristics change significantly. Note that as the reflectivity of the walls increases, higher power levels occur not only in shadowed areas but in LOS positions as well. As expected, the received power increases dramatically (up to 38.16 dB at certain points), while the range of the predictions (the difference between the maximum and minimum values) along the route is 33.75 dB, approximately 20 dB less than the power range with the other conductivity values.

Table V shows the error statistics between the predictions with 0.005 S/m and the other values of wall conductivities. Except for the case of conductive walls, when there is a massive 20.7 dB RMS difference, the variation for the other cases is within logical limits (3.4–4.1 dB). As depicted in Table VI, the mean error with respect to the measurements varies from 3.9 dB to 0.7 dB and the RMS error from 5.2 dB to 3.5 dB as the conductivity values range from 10^{-12} S/m to 0.0005 S/m. Hence, although the wall conductivity notably affects the predictions, the model produces evaluations with acceptable errors in comparison with the measurements for a wide range of values. Furthermore, it can be seen that compared to the measurements, the best predictions are achieved with the value of 0.005 S/m.

B. Sensitivity to the Relative Permittivity of the Walls

Similar analysis to that in the previous section is performed here in order to examine the effect of the relative permitivity of the walls on the predictions. The power results are examined for wall permitivity 3, 3.5, 5, and 7, which are values within the range of permitivity of the building materials in an outdoor environment [12], [13]. Fig. 8 depicts the received power along the route for the above permitivity values and Table VII shows the error statistics in comparison with the results for permitivity 5. The predictions with permitivity 3.5 and 7 are relatively close to the evaluations for $\varepsilon_r = 5$, with RMS errors of 2.3 dB and 3.7 dB, respectively, while the RMS error for $\varepsilon_r = 3$ is 5.45 dB. Generally, as the value of permitivity rises, the received power increases. For the whole route, the mean power for permitivity 3, 3.5, 5 and 7 is -54.84 dBm, -51.53 dBm, -49.84 dBm, and -47.28 dBm, respectively.

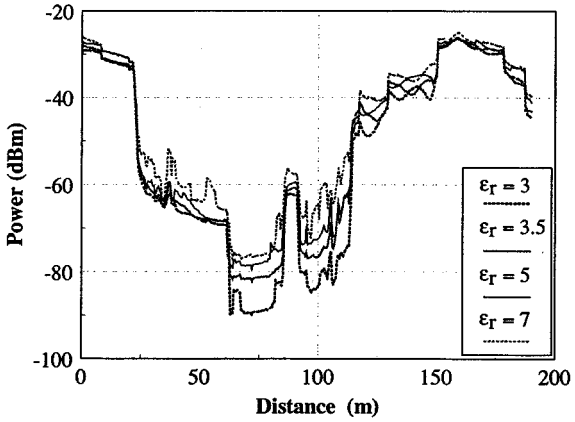

Fig. 8. Power predictions for different values of wall permitively.

TABLE VII
ERROR STATISTICS OF THE POWER RESULTS CONSIDERING VARIOUS WALL PERMITIVITIES WITH RESPECT TO THE PREDICTION WITH $\varepsilon_r = 5$

	Mean error (dB)	RMS error (dB)
$\varepsilon_r = 3$	-4.00	5.45
$\varepsilon_r = 3.5$	-1.69	2.31
$\varepsilon_r = 7$	2.55	3.74

TABLE VIII
ERROR STATISTICS OF THE PREDICTIONS CONSIDERING VARIOUS WALL PERMITIVITIES WITH RESPECT TO THE MEASURED RESULTS

	Mean error (dB)	RMS error (dB)
$\varepsilon_r = 3$	-3.29	6.70
$\varepsilon_r = 3.5$	-0.98	3.98
$\varepsilon_r = 5$	0.71	3.53
$\varepsilon_r = 7$	3.27	4.57

Table VIII shows the error statistics of all the above predictions with respect to the measurements. The RMS errors of the predictions with permitivity 3.5 and 5 are both less than 4 dB (which is in accordance with results presented in [4]). As shown

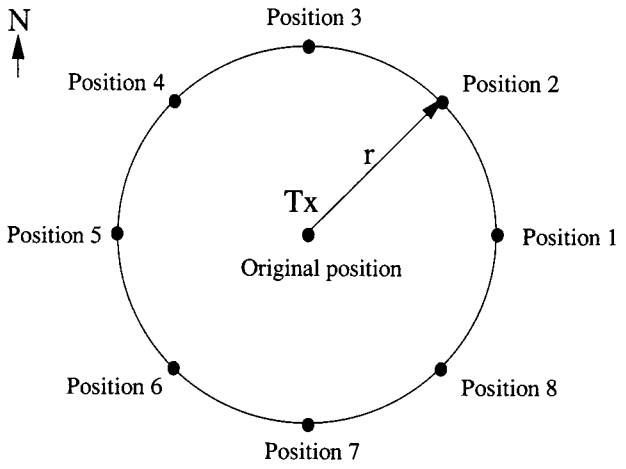

Fig. 9. Studied transmitter positions.

in Table VIII, the worst error in comparison with the measurements is 6.70 dB and occurs for $\varepsilon_r = 3$. The model is most sensitive when the relative permitivity changes from 3 to 3.5. Especially in the deep shadow area between the second and third route corner (∼62–115 m), the effect of the value of permitivity on the predictions is more obvious. For this section of the route, the results with permitivity 3 and 3.5 have an RMS difference of 8.72 dB, and they differ by as much as 13.2 dB at certain points. In the route section between the third and just before the fourth corner (∼115–150 m), where the receiver is moving along a NLOS area with strong reflections, it is obvious that the relation between permitivity and power is not simple and sudden peaks and deeps can appear in the received power due to the change of the reflection coefficient with the changing permitivity and the fluctuation of the total reflection coefficients caused by the addition of the multi-reflected rays inside the wall [9].

V. Sensitivity of the Power Predictions to the Positioning of the Antennas

One of the difficulties in the study of outdoor environments is to accurately map the physical position of the base station and the mobiles to the simulated environment. For this reason, in this section the sensitivity of the power predictions to the correct positioning of the antennas is investigated by changing the transmitting antenna location and analyzing the effects on the channel characteristics. Instead of randomly moving the antenna, the study is performed for specific positions on circles, the center of which is the original transmitter location (Fig. 9). For each circle, eight different positions 45° apart from each other are studied, starting at 0° east from the original location and moving anticlockwise. The same procedure is performed for three circles, with radii (r) 0.5 m, 1 m, and 2 m, respectively. (The 7th position of the circle with 2 m radius is inside the nearby building and hence, it is not considered.) In total, the radio channel is studied for 23 different transmitter positions and compared with the reference channel of the original location, as well as with the results of the field trials.

From the predictions calculated for the 8 positions on the circumference of each circle, the mean received power together with its standard deviation are obtained and shown in Fig. 10. The channel characteristics differ significantly under LOS and NLOS conditions, and hence, as the transmitter moves around, the receiver positions close to the boundaries of the LOS area experience high deviations on their received power (e.g., around 150 m and 175 m). The same behavior is noticed at the boundaries of the illumination zone of strong reflections (e.g., around 120 m and toward the end of the route). However, the most sensitive predictions with respect to the transmitter position are those along the deep shadow sections of the route. This is due to the fact that the rays reaching this area find their way through narrow roads, most of the time under marginal conditions. The larger the radius of the circle of transmitter positions, the wider the areas of large fluctuation and the higher the variance of the results. For $r = 2$ m the deviation is substantial along the entire route, except for the positions directly in front of the transmitter. The total standard deviation for radius 0.5 m and 1 m are close (1.22 dB and 1.82 dB, respectively), but it is almost double for $r = 2$ m (3.39 dB). The mean received powers for r =0.5 and 1 m are also very close to the power of the original position. Similar to the signal deviation, the mean power differs from the original prediction at the receiver positions on the boundaries of the LOS areas and the illumination zone of strong reflections, as well as in the deep shadow areas.

Comparing the received power of all the examined transmitter positions with the results for the original transmitter location, the RMS error along the route for each circle of antenna locations is produced and depicted in Fig. 11. In all cases, the errors are very small directly in front of the transmitter but have large peaks at the boundaries of the LOS area (∼7 dB). For most of the receiver positions the errors for r =0.5 m and r =1 m are very close, while the error for r =2 m is always higher. For each position and for the entire route, the RMS errors with respect to the original position were calculated and found to be less than 2.23 dB, 3.01 dB, and 6.43 dB, for r =0.5 m, 1 m and 2 m, respectively. The total RMS errors are shown in Table IX and are less than 3.7 dB. The total mean errors are small (less than 0.2 dB) because the results fluctuate around the predictions of the original position, as the transmitter moves around this location in a symmetric manner.

In order to examine the error added to the model's predictions due to the antenna misplacement, the simulated results are compared with the mean measurement along the same route. As illustrated in Fig. 12, the error for the original transmitter position and the RMS errors for the transmitter circles with r =0.5 m and 1 m are very close, while for r =2 m the error is larger, especially in the NLOS areas. Most of the peak errors (especially the substantial ones at ∼20 m and 80 m) exist for all configurations, indicating that they are not caused by the inaccurate positioning of the transmitter. The errors due to the movement of the antenna appears to be small as long as the transmitter remains around 1 m from its original location.

The error statistics with respect to the measurements for each position and for the entire route, were also calculated. The RMS errors of all the examined transmitter positions are higher than the error of the central transmitter location, but in most cases, they are close (for r =0.5 m and 1m, the RMS errors differ by less than 0.6 dB). For all the transmitters on the circumference

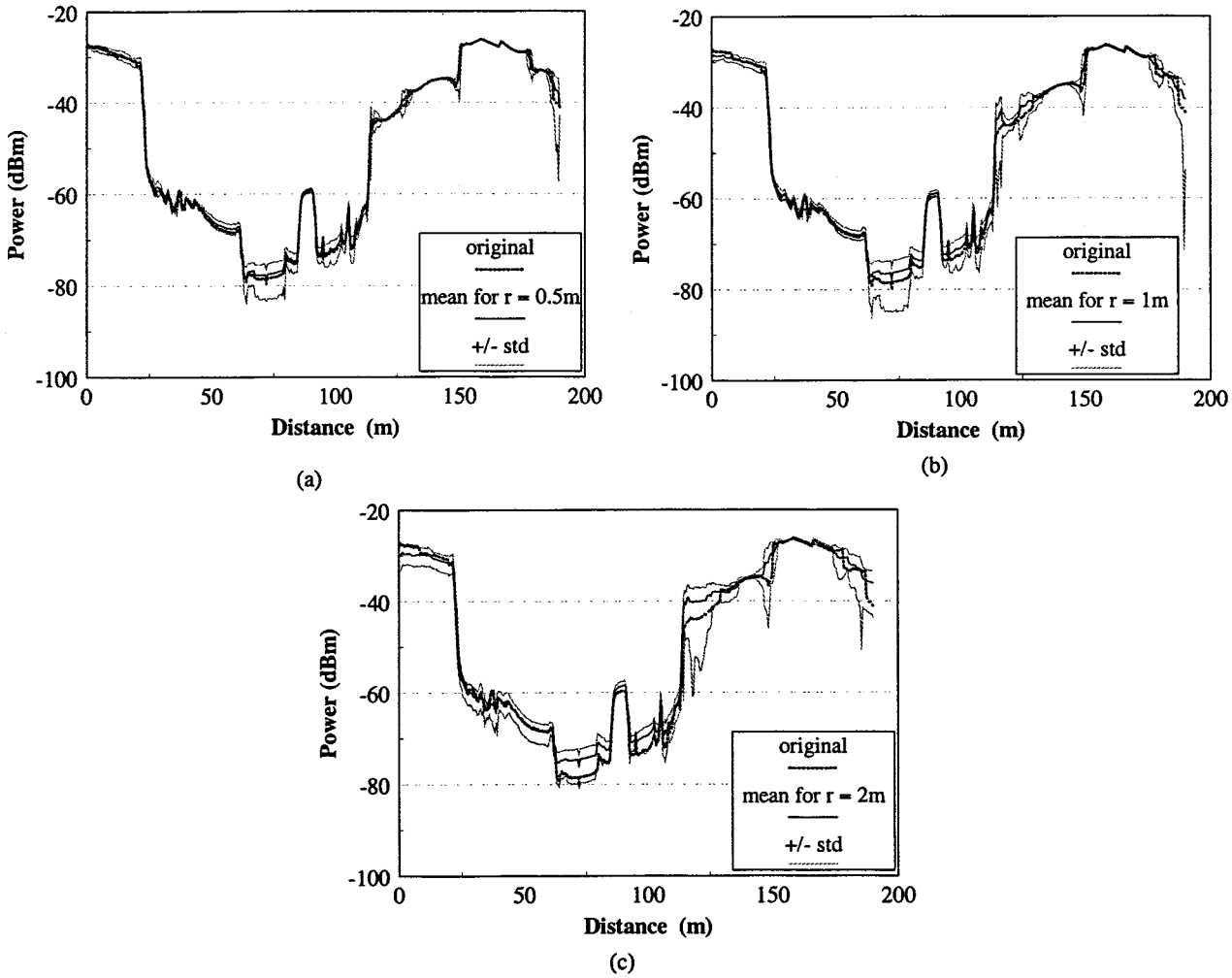

Fig. 10. The mean and the standard deviation of the received power for the transmitter on the circumference of the circles with radius: (a) r =0.5 m, (b) r =1 m, and (c) r =2 m.

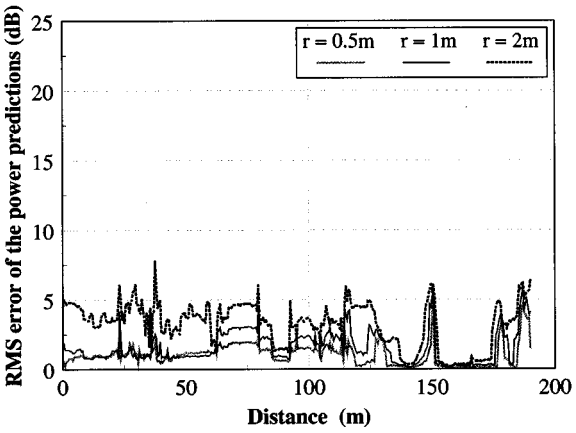

Fig. 11. RMS errors along the route of the three different transmitter circles with respect to the received power of the central transmitter position.

of the circles with r =0.5 m and 1 m, the RMS error with respect to the measured results is smaller than 4.1 dB. For the 2 m radius circle, the worst calculated error was 6.34 dB. As shown in Table X, the total RMS errors for r =0.5 m, 1 m, and 2 m are 3.59 dB, 3.73 dB, and 4.57 dB, respectively. If these values are compared with the 3.48 dB RMS error of the central transmitter

TABLE IX
TOTAL ERRORS OF EACH OF THE THREE DIFFERENT TRANSMITTER CIRCLES WITH RESPECT TO THE RECEIVED POWER OF THE CENTRAL TRANSMITTER POSITION

	Total mean error (dB)	Total RMS error (dB)
r = 0.5m	0.19	1.30
r = 1m	0.19	1.92
r = 2m	0.10	3.60

position, it can be seen that for misplacements of the antenna up to 1 m the predictions of the model are not severely affected. Performance degradation starts occurring when the antenna is moved by more than 1 m, as seen from the RMS errors for the case with $r = 2$ m.

VI. SENSITIVITY TO THE ACCURACY OF THE BUILDING DATABASE

The predictions of the propagation model are limited by the accuracy of the building databases. In this section, the sensitivity

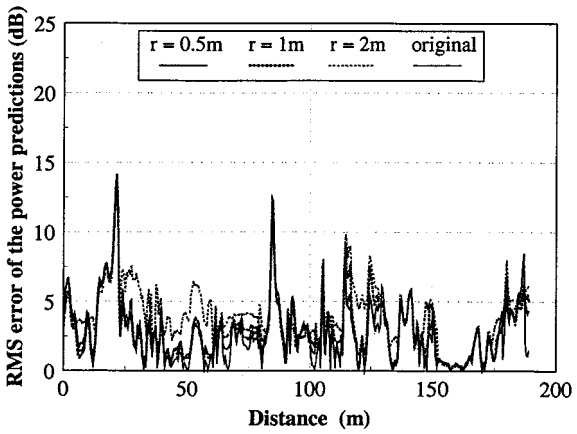

Fig. 12. RMS errors along the route of the three different transmitter circles with respect to the mean measurement.

TABLE X
TOTAL ERRORS OF EACH OF THE THREE DIFFERENT TRANSMITTER CIRCLES WITH RESPECT TO THE MEAN MEASUREMENT

	Total mean error (dB)	Total RMS error (dB)
r = 0.5m	0.90	3.59
r = 1m	0.90	3.73
r = 2m	0.81	4.57
original	0.71	3.53

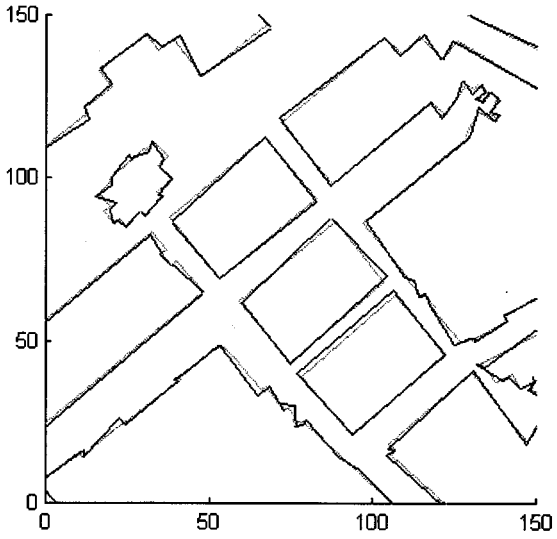

Fig. 13. Part of the original database (grey line) together with a new database (black line) (for $r = 2$ m).

of the outdoor model to the inaccuracies of the input databases is investigated by randomly misplacing the simulated walls and analyzing the effects on the received signal levels. Instead of changing the position and the orientation of each wall independently, the building nodes are moved so that the buildings remain closed polygons (Fig. 13). Each node is displaced by a random distance (from 0 to a predefined r) and toward a random direction. If (x_0, y_0) is the original position of a building node, the new position is (x, y), $x = x_0 + r_0 * \cos(\Theta_0)$ and $y = y_0 + r_0 * \sin(\Theta_0)$, where r_0 is a uniform random number from 0 to r and Θ_0 is a random angle from 0 to 360°. Hence, when the maximum node movement is r, the mean misplacement of the building nodes for the whole database is $r/2$. Four sets of simulations were performed, for databases with up to 0.5 m, 1 m, 2 m, and 3 m node variations. Each set consists of ten route predictions, one for each of the different building databases with the same maximum offset (r). The predictions are obtained along the same predefined route, the only difference being that the receiver positions which (due to the movement of the walls) are now inside a building, are not considered. In total, the radio channel is studied for 40 different building databases and compared with the reference channel of the original configuration and also with the measurements. (For a different approach in the investigation of the sensitivity of a ray based model to the database inaccuracies see [5].)

In Fig. 14, the mean received power together with its standard deviation for each set of predictions with the same maximum displacement (r), are shown. As with the sensitivity to the transmitting antenna position, the receiver locations close to the edges of the LOS area experience high deviations (around 150 m and 175 m), as they lose the LOS with the movement of the walls. The same happens at the boundaries of the illumination zone of strong reflections (e.g., around 120 m and toward the end of the route). Moreover, as the walls change orientation, the focus of the reflected energy also changes, affecting the received power everywhere and especially in the areas where the power is mainly defined by strong reflections (e.g., ∼30 m). Once again, the predictions are most sensitive in the deep shadow sections of the route where most of the time the rays manage to arrive under marginal conditions.

The larger the maximum permitted misplacement of the walls, the wider the area of large fluctuation and the higher the variance of the channel characteristics. For $r = 2$ m the deviation is substantial everywhere except for the positions directly in front of the transmitter. For $r = 3$ m the variation is massive along the entire route. The total standard deviation for r =0.5 m and 1 m are close (1.81 dB and 2.24 dB, respectively), but it almost doubles (in dB) as the maximum displacement becomes 2 m (4 dB) and then 3 m (8.2 dB). As the maximum allowed wall offset increases, the building databases become increasingly dissimilar with each other and their results become uncorrelated. The mean received powers for r =0.5 and 1 m are also close to the power of the original building database. On the contrary, the mean signal levels for $r = 2$ m and 3 m deviate from the original prediction, especially in the deep shadow areas where the deviation at many places is more than 10 dB. In this study, the power generally increases in these areas, as initially the signal was relatively low and the movement of the walls made it easier for more rays to reach this region.

Comparing all the resulting power values with the predictions of the original database, the RMS errors along the route for each set of databases with the same maximum displacement is produced, as depicted in Fig. 15. The errors for all the sets are very small directly in front of the transmitter but have large peaks at the boundaries of the LOS area (∼7 dB). For most of the receiver positions the errors for r =0.5 m and r =1 m are close,

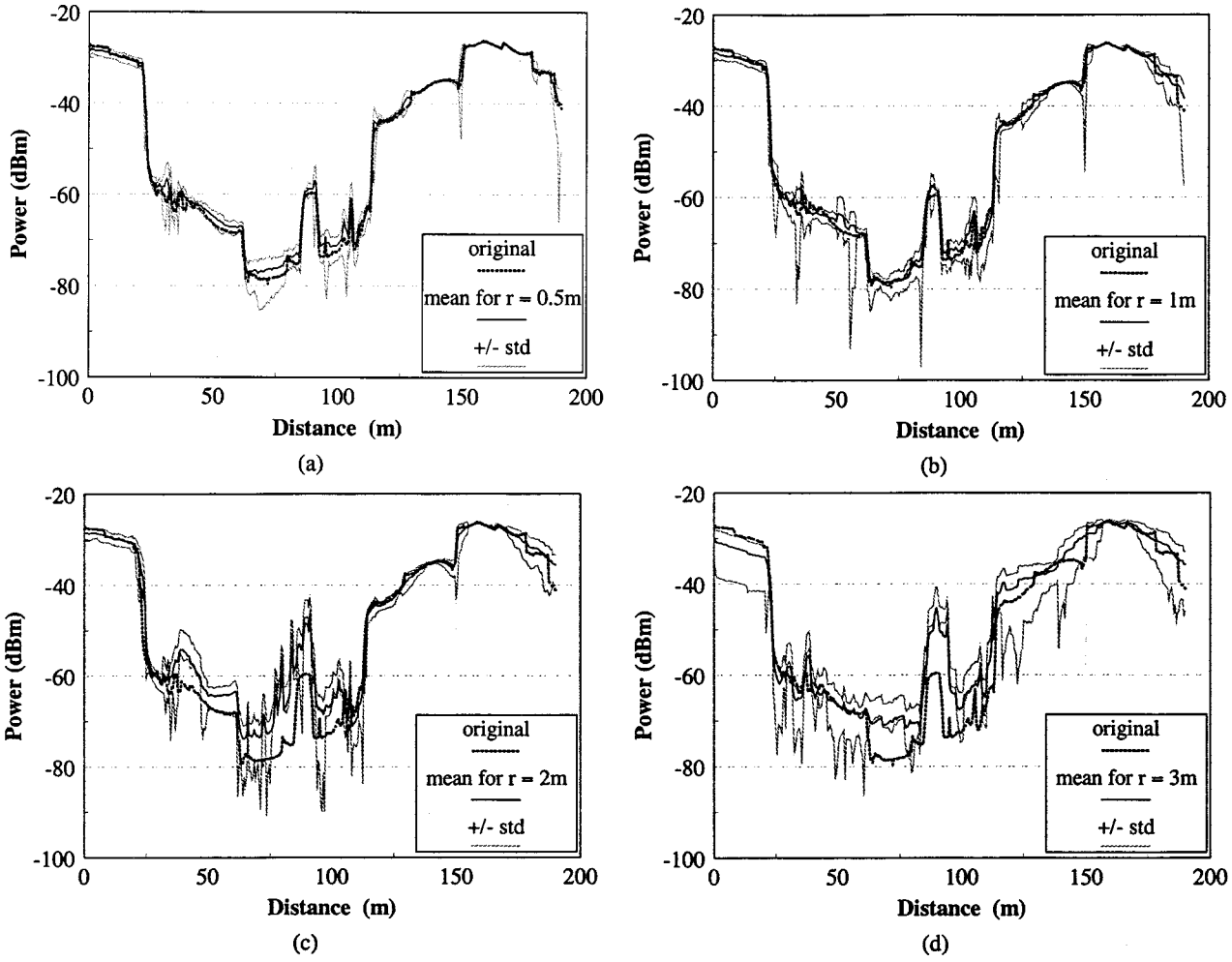

Fig. 14. The mean and the standard deviation of the received power of the ten different building database with maximum displacement (r): (a) 0.5 m, (b) 1 m, (c) 2 m, and (d) 3 m.

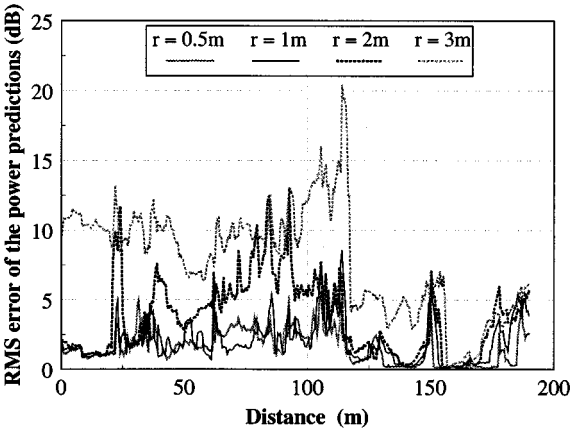

Fig. 15. RMS errors of the power predictions along the route for the four different simulation sets with respect to the received power of the original database.

TABLE XI
TOTAL ERRORS OF THE POWER PREDICTIONS FOR EACH OF THE FOUR DIFFERENT SIMULATION SETS WITH RESPECT TO THE RECEIVED POWER OF THE ORIGINAL DATABASE

	Total mean error (dB)	Total RMS error (dB)
r = 0.5m	0.41	2.03
r = 1m	-0.22	2.51
r = 2m	1.61	4.91
r = 3m	-1.29	8.71

while the error for r =2 m is generally larger (as high as 12 dB) and for r =3 m it becomes significant (up to 20 dB). Due to the random movement of the walls, the error does not increase everywhere as the maximum displacement distance is increasing (e.g., at 70 m the set for r =1 m has smaller RMS error than for r =0.5 m). For each building database and for the entire route, the error statistics with respect to the original received power were calculated. For r =0.5 m and 1 m the RMS errors were found to be smaller than 2.49 dB, but for r =2 m and 3 m they were as high as 7.05 dB and 17.19 dB, respectively. As depicted in Table XI, the total RMS errors for r =0.5, 1, 2, and 3 m are 2.03 dB, 2.51 dB, 4.91 dB, and 8.71 dB, respectively.

Finally, in order to examine the prediction error due to database inaccuracies, the simulated results are also compared with

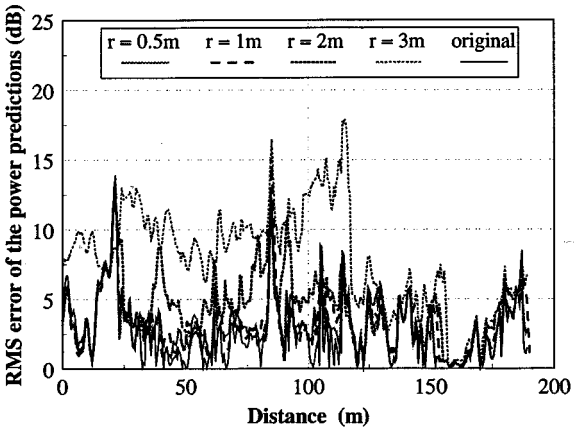

Fig. 16. RMS errors along the route for the four different simulation sets with databases of maximum displacement $r = 0.5$, 1, 2, and 3 m with respect to the measured power.

TABLE XII
TOTAL ERRORS WITH RESPECT TO THE MEASURED POWER FOR EACH OF THE FOUR DIFFERENT SIMULATION SETS WITH DATABASES WITH MAXIMUM OFFSET $r = 0.5$, 1, 2, and 3 m

	Total mean error (dB)	Total RMS error (dB)
r = 0.5m	1.12	3.74
r = 1m	0.48	3.90
r = 2m	0.90	4.61
r = 3m	-2.00	8.70
original	0.71	3.53

the mean measurement along the same route. As illustrated in Fig. 16, the error for the original database and the RMS errors for $r = 0.5$ m and 1 m are close. For $r = 2$ m more error peaks appear, while for 3 m the predictions disagree considerably with the measurements. The large peak errors at 20 m and 80 m exist for all configurations, indicating that they are not caused by the inaccurate wall positions, but they are most probably due to objects or features not included in the simulation (e.g., a large scatterer during the measurements).

The errors with respect to the measurements were also calculated for each of the examined database and for the entire route. For $r = 0.5$ m and 1 m, a couple of databases had slightly smaller RMS error in comparison with the measurements than the original, which was expected since the original database also had an inherent accuracy error. For all databases with $r = 0.5$ m and 1 m, the RMS error with respect to the measured results was smaller than 4.45 dB. For the 2 m maximum displacement, the worst calculated error was 6.32 dB. For $r = 3$ m, apart from a case with 17.31 dB RMS error, the predictions for all other databases had RMS errors less than 9.96 dB. As shown in Table XII, the total RMS errors for $r = 0.5$ m, 1 m, 2 m, and 3 m are 3.74 dB, 3.90 dB, 4.61 dB, and 8.70, respectively. Compared with the 3.48 dB RMS error of the original database, it can be seen that generally, up to 1 m maximum offset the building nodes does not severely affect the model's predictions. However, databases with less accuracy can seriously degrade the performance of the model, as seen from the RMS errors in the case of maximum displacement of 2 m and 3 m.

VII. DISCUSSION—CONCLUSIONS

In this paper the sensitivity of the power predictions of the 3-D ray tracing microcellular model presented in [1], [2] was investigated. The variation of the predictions was examined for different ray permutations, wall characteristics, antenna offsets, and database inaccuracies.

The sensitivity analysis to the maximum permitted ray interactions illustrated that after a certain number of reflections and diffractions, the addition of extra orders did not affect the results, since at each point the predictions converged to a constant value. It was also shown that although at each point only a few of the traced rays contribute to the channel characterization, it is important that the model can handle a very large number of rays, in order to produce reliable results for complex environments, even in deep shadow areas away from the transmitter.

The analysis showed that at LOS positions and in the regions where strong rays existed, a few orders of reflection were adequate to predict the channel characteristics. However, in the deep shadow areas, more reflections and diffractions were needed in order to obtain reliable results. The great importance of diffraction in the modeling of outdoor environments was also illustrated since, despite the considerable complexity that diffraction adds to the model, without this propagation mechanism, the model could not give any predictions for the majority of the NLOS area. For up to seven orders of reflection and two orders of diffraction the predictions were very close to the values of convergence. If the run-time is important, five reflections with one diffraction appeared to be a reasonable compromise for a typical coverage study.

The sensitivity analysis to the conductivity and permitivity of the simulated walls, showed that for the scenario under investigation (a typical urban environment in the center of Bristol), good agreement with the measured power results could be obtained for wall conductivity in the order of 10^{-3} S/m and values of relative permitivity around 5. These results generally agree with findings in [4], although 3-D ray tracing is used here instead of the simpler two-dimensional model of [4].

The sensitivity of the predictions to the correct positioning of the antennas was examined for 23 different transmitting antenna positions on circles, the center of which was the original antenna location. The receiver positions which suffered the highest power deviations were those on the boundaries of the LOS areas, as well as in the deep shadow regions. With respect to the measured results, the RMS errors of all the power predictions with the transmitting antenna 1 m and 2 m away from its original position were less than 4.1 dB and 6.34 dB, respectively. In general, antenna offsets up to 1 m, did not affect the predictions severely.

Finally, the sensitivity of the microcellular model to the inaccuracies in the input building databases was also studied. Four simulation sets with ten runs each were performed, for databases with up to 0.5 m, 1 m, 2 m, and 3 m maximum offset of their

building nodes. As the walls changed orientation, the focus of the reflected energy also altered, affecting the received power everywhere. Also, important rays were obstructed by the displaced walls and others found their way through to areas that they were previously blocked. Once again, the predictions were most sensitive in the deep shadow sections of the route. In comparison with the measured results, the RMS error was smaller than 4.45 dB and 6.32 dB for all databases with node displacement up to 1 m and 2 m, respectively. Hence, building databases with 1 m maximum node offset do not have severe effects on the model's predictions, but less accurate databases can seriously degrade the performance of the model.

ACKNOWLEDGMENT

The authors would like to thank Prof. J. P. McGeehan and Dr. G. V. Tsoulos for their support in many aspects of their research activities. Thanks are also due to Dr. E. Tameh for helpful suggestions.

REFERENCES

[1] G. E. Athanasiadou, A. R. Nix, and J. P. McGeehan, "A microcellular ray-tracing propagation model and evaluation of its narrowband and wideband predictions," *IEEE J. Select. Areas Commun.*, vol. 18, pp. 322–335, Mar. 2000.

[2] ——, "A ray tracing algorithm for microcellular wideband propagation modeling," in *IEEE VTC*, Chicago, IL, July 25–28, 1995, pp. 261–265.

[3] ——, "Comparison of predictions from a ray tracing microcellular model with narrowband measurements," in *IEEE VTC*, Phoenix, AZ, May 4–7, 1997, pp. 800–805.

[4] K. Rizk, J.-F. Wagen, and F. Gardiol, "Two-dimensional ray-tracing modeling for propagation prediction in microcellular environments," *IEEE Trans. Veh. Technol.*, vol. 46, pp. 508–518, May 1997.

[5] ——, "Influence of database accuracy on two dimensional ray tracing based predictions in urban microcells," in *IEEE VTC*, Chicago, IL, July 25–28, 1995, pp. 252–256.

[6] S. S. Wang and J. D. Reed, "Analysis of parameter sensitivity in a ray-tracing propagation environment," in *IEEE VTC*, Chicago, IL, May 4–7, 1997, pp. 805–809.

[7] G. E. Athanasiadou, A. R. Nix, and J. P. McGeehan, "Investigation into the sensitivity of a microcellular ray-tracing model and comparison of the predictions with narrowband measurements," in *IEEE VTC*, Ontario, Canada, May 1998, pp. 870–874.

[8] S. A. Meade, A. R. Nix, and M. A. Beach, "Summary of the processing of the narrowband measurement data for microcells," University of Bristol, Bristol, U.K., Technical Report for the BT VURI project, Aug. 1996.

[9] M. C. Lawton and J. P. McGeehan, "The application of a deterministic ray launching algorithm for the prediction of radio channel characteristics in small-cell environments," *IEEE Trans. Veh. Technol.*, vol. 43, Nov. 1994.

[10] R. J. Luebbers, "Finite conductivity uniform GTD versus knife edge diffraction in prediction of propagation path loss," *IEEE Trans. Antennas Propagat.*, vol. AP-32, pp. 70–76, Jan. 1984.

[11] S. Y. Seidel and T. S. Rappaport, "Site-specific propagation prediction for wireless in-building personal communications system design," *IEEE Trans. Veh. Technol.*, vol. 43, pp. 1058–1066, Nov. 1994.

[12] A. R. Von Hippel, *Dielectric Materials and Applications*. New York: The Technology Press of MIT and Wiley, 1954.

[13] *American Institute of Physics Handbook*, 3rd ed. New York: McGraw-Hill, 1972.

Georgia E. Athanasiadou (M'00) received the M.S. degree in electrical and computer engineering from the National Technical University of Athens, Greece, in 1992 and the Ph.D. degree from the University of Bristol, Bristol, U.K., in 1997.

From October 1996 until October 1999, she was a Research Associate and then a Research Fellow at the Centre for Communications Research, University of Bristol, working in the area of radio propagation modeling. As part of her research she has developed, investigated, and evaluated novel indoor and outdoor ray tracing propagation models. Her research interests include network planning issues with ray tracing models for different air interface techniques, with particular emphasis on adaptive antennas and future generation systems. She is now a Senior Research Engineer with Adaptive Broadband Ltd., Cambridge, U.K. working on broadband systems.

Dr. Athanasiadou is a member of the Technical Chamber of Greece.

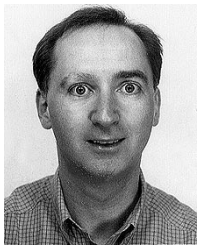

Andrew R. Nix (A'97) was awarded B.Eng. and Ph.D. degrees in electrical and electronic engineering from the University of Bristol, in 1989 and 1993, respectively. Following his Ph.D. he was appointed to a lecturing position at the University of Bristol. In 1999 he was promoted to his current position as Reader in the area of Digital Communications.

His main research interests include wireless propagation, modulation and wireless LANs. He currently heads the propagation modelling and wireless LAN groups in the Centre for Communications Research.

In the area of Wireless LANs, he has managed Bristol's contribution in a number of collaborative European projects. In the area of propagation modelling, his research group has produced leading propagation models based on site specific ray tracing and radar cross section techniques. He has published in excess of 130 journal and conference papers and is a member of ETSI BRAN.